J. Chem. Sci. Vol. 129, No. 2, February 2017, pp. 193–202.
DOI 10.1007/s12039-017-1222-5

REGULAR ARTICLE

Study of behaviour of Ni(III) macrocyclic complexes in acidic aqueous medium through kinetic measurement involving hydrogen peroxide oxidation and DFT calculations

ANURADHA SANKARAN[a,b], E J PADMA MALAR[c,*] and VENKATAPURAM RAMANUJAM VIJAYARAGHAVAN[a,*]

[a]Department of Physical Chemistry, University of Madras, Guindy Campus, Chennai 600 025, India
[b]Department of Chemistry, PSNA College of Engineering and Technology, Kothandaraman Nagar, Dindigul, Tamilnadu 624 622, India
[c]National Centre for Ultrafast Processes, University of Madras, Taramani Campus, Chennai 600 113, India
Email: smradha73@gmail.com; ejpmalar@yahoo.com; viju47@yahoo.co.in

MS received 25 August 2016; revised 20 November 2016; accepted 22 December 2016

Abstract. The Cu(II) ion-catalysed kinetics of oxidation of H_2O_2 by $[Ni^{III}L]$ [where L = L_1 (cyclam) and L_2 (1,8-bis(2-hydroxyethyl)-1,3,6,8,10,13-hexaazacyclotetradecane)] was studied in the pH range of 3.6–5.6 in acetic acid-acetate buffer medium at 25°C in the presence of sulphate ion. The ionic strength (I) was maintained at 0.5 M ($NaClO_4$). The rate constants showed an inverse acid dependence and $[Ni^{III}L_2]$ was observed to be more stable than $[Ni^{III}L_1]$. The rate of the reaction of both complexes with hydrogen peroxide shows contrasting behaviour at pH > 2.5 when compared to the same reaction in perchloric acid medium. DFT calculations performed on the complexes $[Ni^{III}L_1(SO_4)(OAc)]$ and $[Ni^{III}L_2(SO_4)(OAc)]$ reveal that both the acetate and sulphate ligands are axially coordinated to the metal centre. In addition, there is strong hydrogen bonding between the axial ligand and NH hydrogen of the macrocyclic ligand. The computed covalent bond orders in the aqueous medium predict that the acetate forms stronger coordinate bond with Ni ion than the sulphate ligand. The hydroxyl group present in one of the pendant groups of L_2 forms a strong hydrogen bond with the sulphate ligand which leads to additional stability in $[Ni^{III}L_2(SO_4)(OAc)]$.

Keywords. Nickel(III) macrocycle; hydrogen peroxide oxidation; Cu(II); H-bond; DFT calculations.

1. Introduction

Nature chooses macrocyclic complexes due to the enhanced kinetic and thermodynamic stabilities. The redox chemistry of synthetic poly-aza macrocycles explores the properties of nickel containing enzymes.[1] Ni(II)–cyclam derivatives play an important role in receptor recognition.[2] Metal-dioxygen adducts, detected in the catalytic cycles of dioxygen activation by metalloenzymes and biomimetic compounds as key intermediates show a diverse and rich chemistry in structures, spectroscopic properties and reactivities.[3] Tervalent nickel complexes with macrocyclic ligands can be stabilized thermodynamically and kinetically by the binding of anionic axial ligands.[4] The results of Mayerstein and co-workers revealed that the formate ligand plays an ambivalent role both as a reducing agent and as a stabilizer of the trivalent nickel complex.[5] Zilbermann *et al.*, studied the stabilization of Ni(III) in 1,8-dimethyl-1,3,6,8,10,13-hexaazacyclotetradecane by axial binding of anions in neutral aqueous solutions through the formation of $Ni^{III}LX_2$ complexes (where X = F^-, SO_4^{2-}, HPO_4^{2-}, HCO_2^-, $C_6H_5CO_2^-$, $CH_3CO_2^-$ and $(CH_3)_3CCO_2^-$).[4] These complexes were found to be powerful single electron oxidizing agents in aqueous acidic medium.[6–8] Aromatic carboxylates were reported to form intra/intermolecular hydrogen bonding interactions with Ni cyclam complexes and function as good candidates for the construction of multi-dimensional coordination polymers.[9–13]

Metal ion-catalysed decomposition of hydrogen peroxide in acidic and alkaline medium was reported in previous studies.[7,8] Oxidation of hydrogen peroxide by tris(2,2′-bipyridine) and tris(4,4′-dimethyl-2,2′-bipyridine) complexes of osmium(III), iron(III), ruthenium(III), and nickel(III) studied in acidic and neutral aqueous media, showed an inverse acid dependence over the pH range 6.0–8.5.[14] Kinetic measurements with an excess of H_2O_2 revealed that HO_2^- is the only redox-active species for the reaction with $[Ni(tacn)_2]^{3+}$ under conditions 2 < pH < 5.5, while the participation of both H_2O_2 and HO_2^- was observed

*For correspondence

for the reactions with $[Fe(ttcn)_2]^{3+}$ and $[Ru(bipy)_3]^{3+}$.[15] The above work by Takagi and coworkers provides evidence for the dissociation of H_2O_2 into H^+ and HO_2^-.[15] Both H_2O_2 and HO_2^- are found to be reactive oxygen species (ROS) and react with $[Ni^{III}L]$ in absence and presence of stabilizing anions such as sulphate.[7,8]

Recently, we have studied in detail the kinetics of oxidation of hydrogen peroxide by Ni(III) tetra-aza and hexa-aza macrocycles in acidic aqueous solution in the presence of sulphate ion in the pH range 1–2.5.[7,8] We found that the rate of oxidation of H_2O_2 by $[Ni^{III}L_2(SO_4)]^+$ was faster than that by $[Ni^{III}L_1(SO_4)]^+$ below pH 2.5 in the presence and absence of Cu(II) ion. The electronic and geometric structures of tetra-aza and hexa-aza macrocyclic Ni(III) complexes studied by quantum chemical calculations revealed different bonding modes between the nickel ion and the water ligand for $L = L_1$ and L_2.[8] The water molecule binds to Ni(III) in $[NiL_1(SO_4)]^+$ through coordinate bond and the octahedral complex $[Ni^{III}L_1(SO_4)(H_2O)]^+$ is formed. However, in the case of the hexa-aza macrocyclic complex, the water molecule forms only two weak hydrogen bonds with L_2 and leads to the hydrated complex $[Ni^{III}L_2(SO_4)]^+.H_2O$. It is less stable than $[Ni^{III}L_1(SO_4)(H_2O)]^+$ in view of the weak H-bonding interactions between the hydrated water and L_2 and reacts faster. In the present work, we have observed that the rate of oxidation of H_2O_2 by $[Ni^{III}L_1]$ complex increases with pH in the presence of sulphate ion and acetic acid- acetate buffer medium.

Earlier studies have shown that the acetate (OAc) anion can coordinate as a monodentate as well as a bidentate ligand in metal complexes.[16,17] Hunter *et al.*, have shown that the acetate anion coordinates axially as a monodentate ligand in $[Ni^{II}L_1(OAc)_2]\cdot H_2O$.[2] The crystal structure of the above complex shows that the acetate ions are also involved in a network of hydrogen bonding with the water molecules. It is found that in [Ni(benzylcyclam)(OAc)](OAc).$2H_2O$, the macrocycle adopts an unusual folded cis-V configuration with Ni(II) coordination to bidentate acetate. In cyclam-acetato iron complexes the carboxylate group functions as monodentate ligand and is axially coordinated to iron.[18,19] In the presence of suphate ion, acetic acid and sodium acetate buffer, both sulphate and acetate ions can coordinate axially to $Ni^{III}L$, as inferred from the analysis of binding constants reported by Meyerstein and coworkers.[4] To understand the observed kinetics, we have examined the stability of the macrocyclic complexes $[Ni^{III}L_1(SO_4)(OAc)]$ and $[Ni^{III}L_2(SO_4)(OAc)]$, shown in Figure 1, by analysing the structure and bonding using DFT calculations. The low-spin Ni(III) complexes contain one unpaired electron and have doublet ground state.

2. Experimental

2.1 *Materials*

$[NiL_1](ClO_4)_2$, and the corresponding $[NiL_1(NO_3)_2]ClO_4$ complexes were prepared as described previously.[20,21] The UV spectrum of $[NiL_1](ClO_4)_2$ ($\varepsilon_{451} = 48\ M^{-1}\ cm^{-1}$, $\varepsilon_{213} = 12{,}920\ M^{-1}\ cm^{-1}$) in aqueous solution and $[NiL_1(NO_3)_2]ClO_4$ ($\varepsilon_{296} = 11{,}400\ M^{-1}\ cm^{-1}$, $\varepsilon_{370} = 5{,}000\ M^{-1}\ cm^{-1}$) in acidic aqueous solution in the presence of sulphate were recorded. $[Ni^{II}L_2](ClO_4)_2$ and the corresponding $[NiL_2(Br_2)]ClO_4\cdot 2H_2O$ complex were prepared as described previously.[6,22,23] The UV spectra of $[NiL_2](ClO_4)_2$ in aqueous solution ($\varepsilon_{444} = 54\ M^{-1}\ cm^{-1}$, $\varepsilon_{205} = 15{,}300\ M^{-1}\ cm^{-1}$) and the Ni(III) complex in acetonitrile ($\varepsilon_{381} = 7500\ M^{-1}\ cm^{-1}$, $\varepsilon_{291} = 10{,}600\ M^{-1}\ cm^{-1}$) were taken. ESR spectra of both Ni(III) complexes in aqueous acidic medium in the presence of excess sulphate at 77 K were used for characterising the

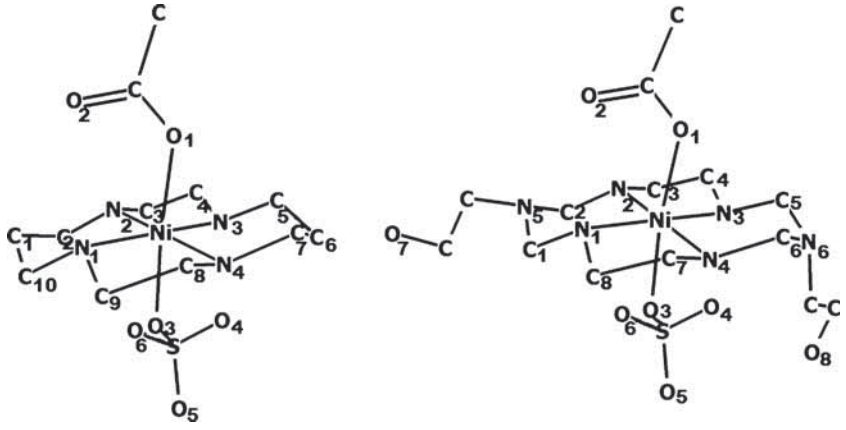

Figure 1. Structure of the complexes studied with the atomic labelling in the macrocyclic and axial ligands.

complexes. The EPR spectra of the complexes with $g_\perp$ values greater than the $g_{||}$ indicate that the Ni(III) are in low spin state with tetragonally distorted octahedral geometry and that nickel complexes are no longer square-planar. The Ni(III) solution was prepared freshly by dissolving the sample in aqueous acidic solution containing sulphate for stabilizing the Ni(III). A stock solution of acetic acid was prepared by dilution of glacial acetic acid (Analar grade) and standardized using sodium hydroxide which in turn was standardized using potassium hydrogen phthalate. Sodium acetate solution was prepared by weight. The pH was measured with a Eutech India pH meter. Sodium perchlorate (Loba Chemie, India) was purchased and used as such to maintain the ionic strength. A stock solution of copper perchlorate was prepared by neutralizing copper carbonate (0.0091 mol, 2 gram) with 70% perchloric acid (1.56 mL, 0.018 mol). The resultant solution was standardized iodometrically.

Caution: Compounds containing perchlorate anions must be regarded as potential explosives and should be handled with caution.

2.2 *Kinetic studies*

Kinetics of oxidation of hydrogen peroxide by $[NiL_1(SO_4)]^+$ and $[NiL_2(SO_4)]^+$ were studied under second and first order conditions in the presence of sulphate ion. The ionic strength was maintained at 0.5 mol dm^{-3} using sodium perchlorate. The concentration of $[H_2O_2]$ was varied from 2.5×10^{-4} to 1×10^{-3}mol dm^{-3} and the Ni(III) complex concentration was fixed at 5×10^{-5} mol dm^{-3}. The concentration of [Cu(II)] was fixed at 1×10^{-4} and 5×10^{-6} mol dm^{-3}. The effect of sulphate on the reaction rate was studied by varying its concentration at 0.01 and 0.02 mol dm^{-3}. The pH dependence on the reaction rate was studied by varying the pH between 3.6–5.6 using acetic acid and sodium acetate buffer. Absorbance changes with time were measured using a UV-Visible recording spectrophotometer (Shimadzu UV-1601). Decrease in absorbance of LMCT band of Ni(III) was followed at 350 nm. The observed rate constant k_{obs} was calculated from the slopes of the linear regression plots of $\ln\{1+(Y_o-Y_\infty)\Delta_o/(Y_t-Y_\infty)[A]_o\}$ (where $\Delta_o = a[B_o]-b[A_o]$, A_o and B_o are initial concentrations of oxidant and reductant, respectively) against time for second order and $\ln(Y_t-Y_\infty)$ against time for first order conditions.[24] Y_o and Y_∞ denote the initial and final absorbance of the oxidant and Y_t is the absorbance at time t.

2.3 *Computational aspects*

The nature of bonding in the low-spin nickel complexes, **1** $[Ni^{III}L_1(SO_4)(OAc)]$ and **2** $[Ni^{III}L_2(SO_4)(OAc)]$, were investigated using DFT computations. We studied the above complexes by complete structural optimization with the BP86 functional[25] using Aldrich's extended Triple zeta valence basis set def2-TZVP[26] including the auxiliary def2-TZVP/J basis set. The BP86 functional is found to be suitable to study transition metal chemistry.[8,27,28] We employed the combination of the resolution of the identity (RI) and the "chain of spheres exchange" algorithms (RIJCOSX).[29–33] The computations were carried out using the ORCA 3.0.3 software.[34]

We have performed the computations on the complexes **1** and **2** in aqueous medium using the COSMO method[35] which approximates the solvent surrounding the solute molecule by a dielectric continuum. The third generation dispersion correction with Becke-Johnson damping (D3BJ) was applied to take into account the dispersion interactions acting in the complexes.[36] Nature of the bonding between the nickel ion and the ligands was analysed using Mayer bond order.[37] The complexes in the gas-phase were also studied at BP86/def2-TZVP level using the ORCA 3.0.3 software[34] and at BP86/TZVP level without inclusion of dispersion correction by Gaussian software G03W.[38]

3. Results and Discussion

The stability and redox properties of Ni(III) macrocyclic complexes, $[Ni^{III}L_1]$ and $[Ni^{III}L_2]$ by reaction of trivalent metal complexes with hydrogen peroxide in aqueous acidic medium in the pH range of 1–2.5 were studied earlier.[7,8] In highly acidic medium, oxidation of hydrogen peroxide by $[Ni^{III}L]$ was found to be very slow and complicated by the ligand oxidation. The peroxy anion, HO_2^-, formed by dissociation of hydrogen peroxide (eq. 1) may react with metal complex to form a stable oxidant $[Ni^{III}LHO_2^-]$.

$$H_2O_2 \overset{K_a}{\rightleftharpoons} H^+ + HO_2^- \quad (1)$$

The complexes are stabilized in presence of sulphate in perchloric acid medium. In sulphate medium, $[Ni^{III}L]$ exist as sulphato-complex according to the equation (2)

$$[Ni^{III}L]^{3+} + SO_4^{2-} \overset{K_f}{\rightleftharpoons} [Ni^{III}LSO_4]^+ \quad (2)$$

The metal centred redox reaction takes place in preference to the ligand oxidation in presence of copper ion. On comparing the rate of oxidation of both Ni^{III} complexes in presence of sulphate in the pH range 1–2.5, $[Ni^{III}L_2]$ show higher rate constant even with twice the concentration of sulphate than the $[Ni^{III}L_1]$ (Table 1).[8] In the present work, the kinetics was followed in the pH range 3.6 to 5.6 in the presence of higher sulphate (0.01–0.02 mol dm^{-3}) concentration in order to study the effect of pH on the rate of the reaction.

At higher pH, the decomposition *via* HO_2^- is the preferable path. Since most of the reactions involving hydrogen peroxide are carried out at higher pH (pH > 5), HO_2^- plays an important role and is responsible for the decomposition of H_2O_2. Interaction of [Cu(II)]

Table 1. Comparison of rate constants of Ni(III) complexes at various pH. $[Ni^{III}L] = 5 \times 10^{-5}$ mol dm^{-3}; $[H_2O_2] = 2.50 \times 10^{-5}$ mol dm^{-3}; [Cu(II)] = 1×10^{-4} mol dm^{-3}; T = 25°C; I = 0.50 mol dm^{-3} ($NaClO_4$); pH = 1–2.5 - perchloric acid medium; pH = 3.6–5.6 - acetate buffer.

	$[Ni^{III}L_1]$		$[Ni^{III}L_2]$	
pH	$[Na_2SO_4]$/mol dm^{-3}	K′ / dm^3 mol^{-1} s^{-1}	$[Na_2SO_4]$/mol dm^{-3}	K′/dm^3 mol^{-1} s^{-1}
1.0	0.002[7]	17.0 ± 0.02	0.005	20.3 ± 0.02
1.5	0.002	26.5 ± 0.03	0.005	41.5 ± 0.01
2.0	0.002	36.0 ± 0.03	0.005	60.0 ± 0.01
2.5	0.002	104 ± 0.01	0.005	160 ± 0.03
3.6	0.01	60.5 ± 0.07	0.01	52.1 ± 0.05
4.6	0.01	87.1 ± 0.08	0.01	65.0 ± 0.05
5.0	0.01	110 ± 0.05	0.01	78.0 ± 0.05
5.6	0.01	221 ± 0.02	0.01	134 ± 0.01

with $[Ni^{III}L_2]$ complexes in aqueous acidic condition was ruled out.[7] In aqueous acidic medium, formation of highly labile species $Cu^{I}H_2O_2^{\bullet+}$ and successive electron transfer reaction with $[Ni^{III}L]$ is given by rate equations 3 and 4. For the sake of clarity, the tetra-aza (L_1) and hexa-aza (L_2) macrocyclic ligands are generalised and denoted as L in the rate equations. Further, the acetate and sulphate ligands are not explicitly shown.

$$Cu^{II} + H_2O_2 \overset{K_1}{\rightleftharpoons} Cu^{I}H_2O_2^{\bullet+} \quad (3)$$

$$[Ni^{III}L]^+ + Cu^{I}H_2O_2^{\bullet+} \xrightarrow{k_1} [Ni^{II}L] + Cu^{II} + H_2O_2^{\bullet+} \quad (4)$$

The peroxy anion (HO_2^-) may react with Cu(II) (eq. 5) and the $[Cu^{II}HO_2^-]$ or $[Cu^{I}HO_2^{\bullet}]$ reacts with $[Ni^{III}L(SO_4)]^+$. The rate equation for the Cu(II) ion-promoted peroxy anion may be given by the Equation (6).

$$Cu^{II} + HO_2^- \overset{K_2}{\rightleftharpoons} Cu^{I}HO_2^{\bullet} \quad (5)$$

$$[Ni^{III}L]^+ + Cu^{I}HO_2^{\bullet} \xrightarrow{k_2} [Ni^{II}L] + Cu^{II} + HO_2^{\bullet} \quad (6)$$

The rate expression for the oxidation of H_2O_2 by $[Ni^{III}L]$ may be displayed by the following steps:

$$\frac{-d[Ni^{III}L]}{2dt} = k_1K_1[Ni^{III}L][H_2O_2][Cu^{II}] + k_2K_2K_a[Ni^{III}L][H_2O_2][Cu^{II}]/[H^+] \quad (7)$$

$$k = k_1K_1[Cu^{II}] + k_2K_2K_a[Cu^{II}]/[H^+] \quad (8)$$

$$k = k_a + K_ak_b/[H^+]) \quad (9)$$

The rate constants displayed an inverse acid dependence as shown in Figures 2 and 3 and Table 2. In the rate law equation (9), k_a (= $k_1K_1[Cu^{II}]$) and k_bK_a (k_b = $k_2K_2[Cu^{II}]$) were obtained from the intercept and slope, respectively, of the plot of k against $[H^+]^{-1}$. We observed that rate of oxidation of hydrogen peroxide is almost similar at pH 3.6 for both the complexes and varies significantly at higher pH (Tables 1 and 2).

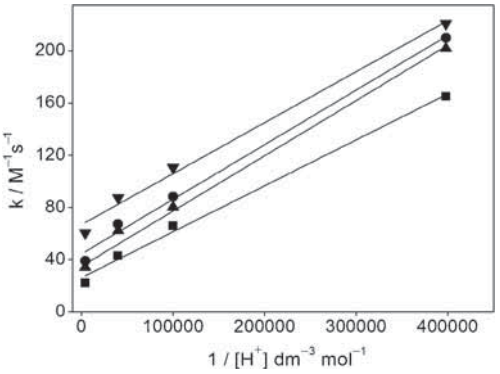

Figure 2. Plot of k against 1/[H^+]; T = 25°C; $[H_2O_2] = 2.50 \times 10^{-4}$ mol dm^{-3}; $[Ni^{III}L_1] = 5 \times 10^{-5}$ mol dm^{-3}; I = 0.50 mol dm^{-3} ($NaClO_4$); $[Na_2SO_4]$ = 0.02 mol dm^{-3} – [Cu(II)]/mol dm^{-3}: ■ - 5×10^{-6} & ● - 1×10^{-4}; $[Na_2SO_4]$ = 0.01 mol dm^{-3} – [Cu(II)] / mol dm^{-3} : ▲ - 5×10^{-6} & ▼ - 1×10^{-4}.

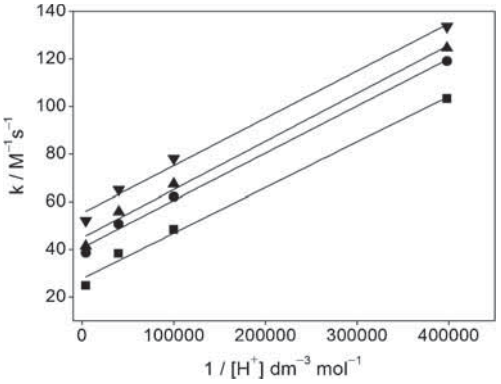

Figure 3. Plot of k against 1/[H^+]; T = 25°C; $[H_2O_2] = 2.50 \times 10^{-4}$ mol dm^{-3}; $[Ni^{III}L_2] = 5 \times 10^{-5}$ mol dm^{-3}; I = 0.50 mol dm^{-3} ($NaClO_4$); $[Na_2SO_4]$ = 0.02 mol dm^{-3} – [Cu(II)]/mol dm^{-3}: ■ - 5×10^{-6} & ● - 1×10^{-4}; $[Na_2SO_4]$ = 0.01 mol dm^{-3} – [Cu(II)]/mol dm^{-3}: ▲ - 5×10^{-6} & ▼ - 1×10^{-4}.

Above pH 3.6, the rate constant for $[Ni^{III}L_1]$ was found to increase when compared with that of $[Ni^{III}L_2]$ at the same reaction condition.

Table 2. Dependence of rate on [Cu(II)] and [Na_2SO_4] at various pH. [$Ni^{III}L$] = 5×10^{-5} mol dm^{-3}; [H_2O_2] = 2.50×10^{-5} mol dm^{-3}; T = 25°C; I = 0.50 mol dm^{-3} ($NaClO_4$).

pH	[Na_2SO_4]/ mol dm^{-3}	[Cu(II)]/ mol dm^{-3}	[$Ni^{III}L_1$] $K'/dm^3\ mol^{-1}\ s^{-1}$	[$Ni^{III}L_1$] $k_bK_a/[H^+]$	[$Ni^{III}L_2$] $k'/dm^3\ mol^{-1}\ s^{-1}$	[$Ni^{III}L_2$] $k_bK_a/[H^+]$
3.6	0.01	5×10^{-6}	34.2 ± 0.04 (36.4)	1.68	41.4 ± 0.04 (45.6)	0.80
		1×10^{-4}	60.5 ± 0.07 (67.1)	1.56	52.1 ± 0.05 (56.0)	0.79
	0.02	5×10^{-6}	21.9 ± 0.06 (27.5)	1.40	24.8 ± 0.05 (28.5)	0.76
		1×10^{-4}	39.0 ± 0.07 (46.1)	1.67	38.5 ± 0.04 (41.5)	0.79
4.6	0.01	5×10^{-6}	62.1 ± 0.08 (52.1)	16.8	55.7 ± 0.04 (52.9)	8.04
		1×10^{-4}	87.1 ± 0.08(81.6)	15.6	65.0 ± 0.05 (63.1)	7.93
	0.02	5×10^{-6}	42.9 ± 0.04 (40.4)	14.0	38.2 ± 0.04 (35.3)	7.60
		1×10^{-4}	67.3 ± 0.07 (61.2)	16.7	50.7 ± 0.03 (48.6)	7.88
5.0	0.01	5×10^{-6}	80.3 ± 0.04 (77.3)	42.3	67.3 ± 0.02 (65.1)	20.2
		1×10^{-4}	110 ± 0.05 (106)	39.1	78.0 ± 0.05 (75.1)	19.9
	0.02	5×10^{-6}	65.7 ± 0.05 (61.2)	35.2	48.3 ± 0.03 (46.9)	19.1
		1×10^{-4}	88.4 ± 0.04 (86.3)	41.9	62.0 ± 0.03 (60.6)	19.8
5.6	0.01	5×10^{-6}	202 ± 0.01 (203)	168	124 ± 0.02 (125)	80.4
		1×10^{-4}	221 ± 0.02 (222)	156	134 ± 0.01 (134)	79.3
	0.02	5×10^{-6}	165 ± 0.02 (166)	140	103 ± 0.01 (103)	80.4
		1×10^{-4}	210 ± 0.02 (211)	167	119 ± 0.01 (119)	78.8

Note: Numbers in parentheses are values calculated by use of equation (9).

This trend is just opposite to that observed for lower pH 1–2.5 (Table 1). Above pH 5, the influence of Cu(II) was studied by carrying out the oxidation of hydrogen peroxide by [$Ni^{III}L_1$] complex at pH 5.6 and sulphate concentration of 0.01 mol dm^{-3}, in the absence of Cu(II). We found that the rate constant was 170 $dm^3mol^{-1}\ s^{-1}$ which is less than that of the same reaction in the presence of Cu(II) (Table 2).

3.1 *Structure and Bonding in the Ni(III) macrocyclic complexes [$Ni^{III}L_1(SO_4)(OAc)$] and [$Ni^{III}L_2(SO_4)(OAc)$]*

Figures 4 and 5 show the optimized geometries of the complexes **1** and **2**, as predicted by the BP86/def2-TZVP calculations in aqueous medium and gas phase, respectively.

For clarity, we have omitted the hydrogen atoms other than the ones involved in hydrogen bonding. The

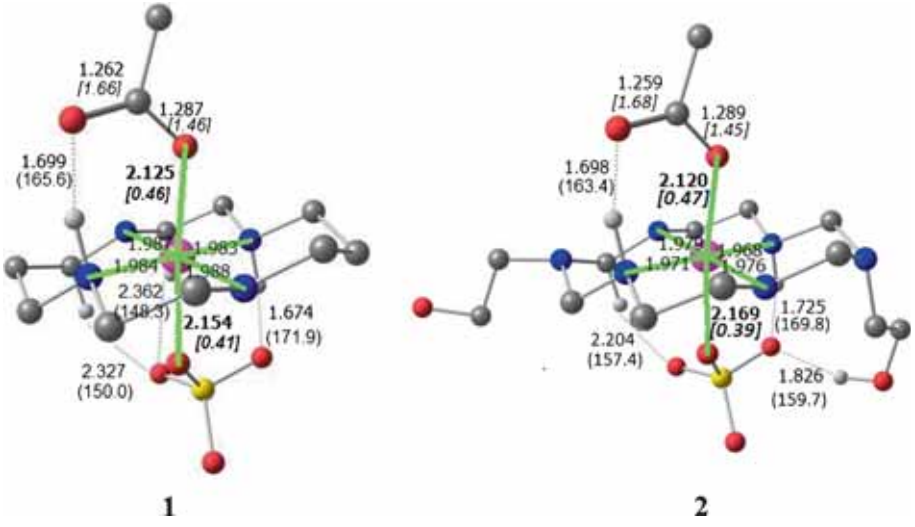

Figure 4. BP86/def2-TZVP optimzed geometries of Ni(III) acetate complexes **1** and **2** in aqueous medium. Hydrogen atoms forming hydrogen bonds alone are shown for clarity. Hydrogen bonds are denoted by dotted lines. Hydrogen bond lengths in Å and hydrogen bond angles in degrees (inside parenthesis) are given. The coordinate bonds are marked in green along with their bond lengths. The axial coordinate bond lengths are in bold and the corresponding covalent bond orders are given inside square brackets in italics. Color code for atoms: H – white; C – grey; N – blue; O – red; S – yellow; Ni – purple.

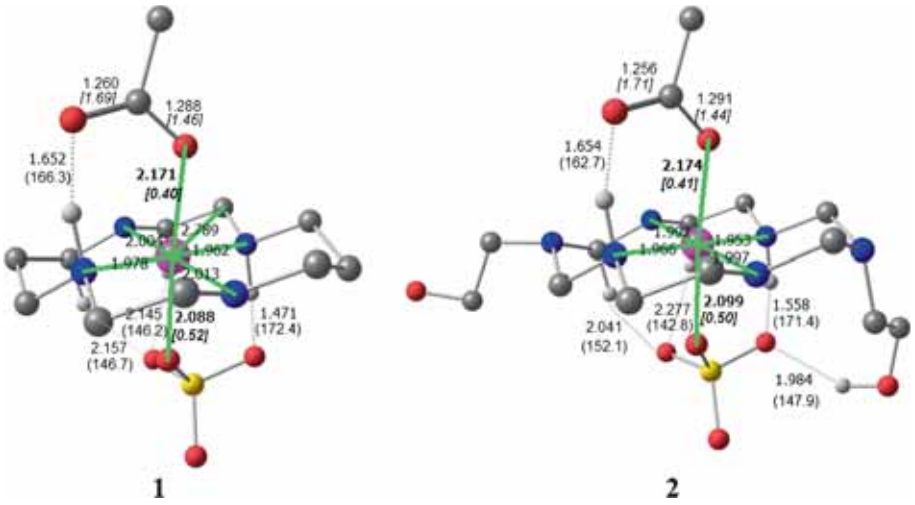

Figure 5. BP86/def2-TZVP optimzed geometries of Ni(III) acetate complexes **1** and **2** in gas-phase. Hydrogen atoms forming hydrogen bonds alone are shown for clarity. Hydrogen bonds are denoted by dotted lines. Hydrogen bond lengths in Å and hydrogen bond angles in degrees (inside parenthesis) are given. The coordinate bonds are marked in green along with their bond lengths. The axial coordinate bond lengths are in bold and the corresponding covalent bond orders are given inside square brackets in italics. Color code for atoms: H – white; C – grey; N – blue; O – red; S – yellow; Ni – purple.

complete optimized geometries in the aqueous medium are given in Supporting Information (Figure S1). The present structural optimization reveals that the macrocyclic ligands L_1 and L_2 adopt trans-III configuration as observed earlier.[8] Selected bond lengths, bond angles and dihedral angles for the above octahedral complexes are given in Table 3. The DFT study predicts Ni^{III}–N equatorial bond lengths of 1.983–1.987 Å in the Ni cyclam complex **1** $[Ni^{III}L_1(SO_4)(OAc)]$. These bond lengths are similar to the values of 1.977–1.996 Å predicted in the corresponding aqua complex $[Ni^{III}L_1(SO_4)(H_2O)]^+$ at the same computational level.[8] In the hexa-aza macrocyclic complex **2** $[Ni^{III}L_2(SO_4)(OAc)]$, the Ni^{III}–N bond lengths are shortened by about 0.01 Å and are in the range 1.968–1.979 Å. The above equatorial Ni–N coordinate bond lengths agree closely with the mean equatorial Ni–N distance of 1.973 ± 0.006 Å observed in $[Ni^{III}L_1(NO_3)_2]^+$.[21] Though the Ni–N bond lengths in **2** are shorter than that in **1** by about 0.01 Å, the computed covalent bond orders of the equatorial bonds are very similar in both complexes **1** and **2**. Table 3 shows that the equatorial Ni–N coordinate bonds in **1** and **2** exhibit covalent bond order in the range 0.61–0.69. The axial Ni–O bond lengths involving the sulphate ligands are 2.154 and 2.168 Å, respectively, in complexes **1** and **2** while the corresponding Ni–O bond lengths between the axial acetate ligand and Ni(III) are 2.125 and 2.121 Å. The significant shortening of ~0.03 and 0.05 Å in the axial Ni–O bond lengths in the case of the acetate ligand reveals that the coordinate bond between acetate ligand and Ni(III) is stronger than that between the sulphate and Ni(III) in the aqueous medium. This is substantiated by the computed covalent bond orders 0.46 and 0.47 for the acetate ligand in $[Ni^{III}L_1(SO_4)(OAc)]$ and $[Ni^{III}L_2(SO_4)(OAc)]$, respectively, whereas the corresponding bond orders for the sulphate ligand are 0.41 and 0.39. The predicted Ni–O(acetate) axial bond lengths in **1** and **2** are about 0.02 Å longer than the corresponding observed length of 2.106 Å in the crystal structure of $[Ni^{II}L_1(OAc)_2]\cdot H_2O$.[2] It is seen that in the complexes under study the axial bonds have covalent bond orders < 0.5. Similar observation was made earlier in some octahedral complexes and other transition metal complexes.[8,39–42]

Though the present analysis reveals that the acetate anion is more strongly bound to the Ni(III) than the sulphate anion in the aqueous medium, the gas-phase calculations show the reverse trend (Table 3 and Figure 5). In the gas-phase, the Ni-sulphate coordinate bonds have bond orders of 0.52 and 0.50 in **1** and **2**, respectively, while the bond orders are 0.40 and 0.41 for the corresponding Ni-acetate bonds (Table 3 and Figure 5). The Frontier Molecular orbitals in **1** and **2** as obtained by gas-phase BP87/TZVP calculation are depicted in Figures 6 and 7. The presence of the two hydroxy ethyl groups in the tetra-aza complex **2**, has raised the highest occupied MO (HOMO) energy and lowered the lowest

Table 3. Selected structural parameters in the complexes **1** and **2** in aqueous medium optimized at BP86/def2-TZVP level. The values inside parentheses in italics correspond to covalent bond orders.

	Aqueous medium-COSMO		Gas-phase	
Parameter	**1**	**2**	**1**	**2**
Bond lengths in Å (*bond orders*)				
Ni-N1	1.984 *(0.68)*	1.971 *(0.69)*	1.978 (0.66)	1.966 *(0.66)*
Ni-N2	1.987 *(0.67)*	1.979 *(0.68)*	2.004 *(0.65)*	1.992 *(0.65)*
Ni-N3	1.983 *(0.69)*	1.968 *(0.69)*	1.962 *(0.71)*	1.953 *(0.71)*
Ni-N4	1.987 *(0.61)*	1.976 (0.62)	2.014 *(0.56)*	1.997 *(0.59)*
Ni-O1	2.125 *(0.46)*	2.121 *(0.47)*	2.171 *(0.40)*	2.174 *(0.41)*
Ni-O3	2.154 *(0.41)*	2.168 *(0.39)*	2.088 *(0.52)*	2.099 *(0.50)*
N1-N2	2.890	2.865	2.896	2.882
N3-N4	2.909	2.906	2.915	2.900
N2-N3	2.715	2.698	2.711	2.697
N1-N4	2.712	2.690	2.725	2.700
Hydrogen bond lengths in Å (*bond orders*)				
O3-HN1	1.699 *(0.17)*	1.698 *(0.16)*	1.652 *(0.19)*	1.654 *(0.19)*
O4-HN3	1.674 *(0.15)*	1.725 *(0.12)*	1.471 *(0.27)*	1.558 *(0.21)*
O4-HO8	–	1.826 *(0.10)*	–	1.984
O6-HC2	2.327	2.204	2.157	2.041
O6-HC3	2.362	–	2.145	2.277
Bond angles and dihedral angles (°)				
N1-Ni-N2	93.4	93.0	93.3	93.5
N3-Ni-N4	94.2	94.9	94.3	94.5
N2-Ni-N3	86.3	86.3	86.3	86.2
N4-Ni-N1	86.1	85.9	86.1	85.9
N1-N2-N3	90.1	90.1	89.2	89.2
N1-N2-N3-N4	–0.4	–1.1	–0.5	–1.3
Ni-N1-N2-N3	0.5	0.7	0.6	0.7

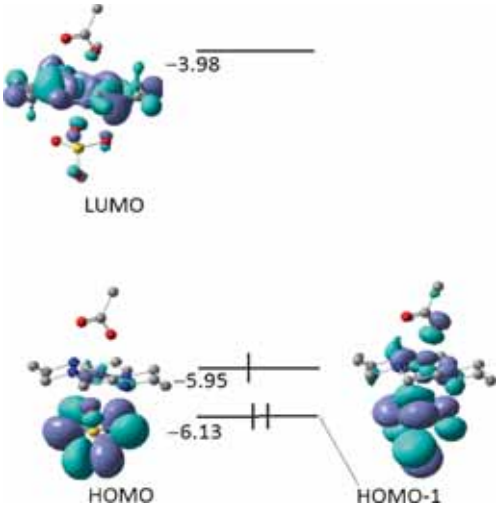

Figure 6. Frontier Molecular Orbitals and the energies of the α -spin MOs (in eV) of [$Ni^{III}L_1(SO_4)(OAc)$]].

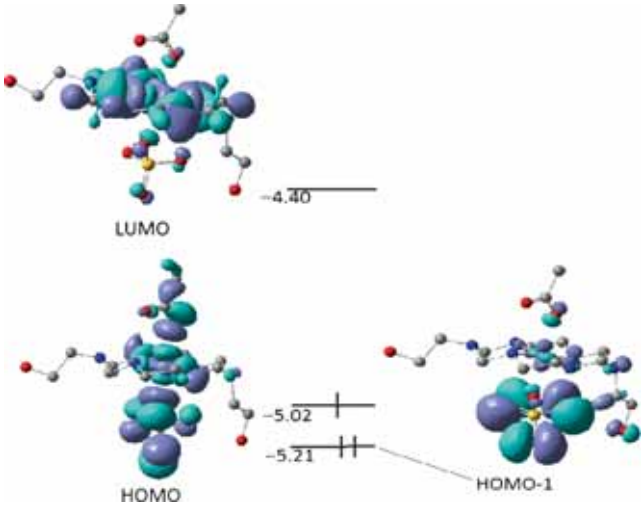

Figure 7. Frontier Molecular Orbitals and the energies of the α-spin MOs (in eV) of [$Ni^{III}L_2(SO_4)(OAc)$]].

unoccupied MO (LUMO) energy. It is seen that the HOMO and HOMO-1 have small energy difference of about 0.2 eV in **1** and **2**.

Both these occupied MO's have dominant contribution from the sulphate oxygen atoms and it is observed that the there is a reversal of order in the two complexes. Thus, the HOMO in **1** and HOMO-1 in **2** have identical nature. The LUMO is delocalized over the coordinating nitrogen atoms of the macrocyclic ligand and the Nickel atom in both the complexes.

In addition to the formation of axial coordinate bonds in **1** and **2**, the acetate and sulphate ligands also form hydrogen bond (H-bond) with the macrocyclic ligand L. Thus, the acetate oxygen labelled O_2 in Figure 1 forms H-bond with the secondary hydrogen, N_1H, of

L. Similarly, the sulphate oxygen O_4 (Figure 1) forms H-bond with the hydrogen of N_3H. These hydrogen bonds, depicted in Figure 4 with dotted lines, have short lengths in the range 1.674–1.725 Å and H-bond angles in the range of 163–172°, and these are strong H-bonds.[43] These H-bonds have significant covalent character as reflected by the Meyers bond order in the range 0.12–0.17 (Table 3). Besides the above H-bonds that are common in both complexes **1** and **2**, an additional H-bond is formed in **2** due to the presence of pendant hydroxyethyl group bonded to the tertiary nitrogen atom N_6. The hydrogen of this OH forms H-bond with the sulphate oxygen O_4 having a length 1.826 Å and H-bond angle 159.7°. This H-bond also has significant covalent bond order of 0.10 and is strong. We have also identified two weak hydrogen bonds ($O_6 \ldots HC_2$ and $O_6 \ldots HC_3$) between the oxygen atom O_6 of sulphate and the CH hydrogens of L_1 in **1** as shown in Figure 3. However, in **2** only one weak H-bond $O_6 \ldots HC_2$ is formed.

Though the formation of coordinate bond and H-bond by the axial acetate as well as sulphate ligands described above is similar in the complexes **1** and **2**, we have observed different trends in the reaction kinetics at various pH (Table 1). It is of interest to compare that our earlier study on $[NiL_1(SO_4)(H_2O)]^+$ at the same computational level showed that the aqua ligand is coordinated to Ni(III) with Ni–O covalent bond order of 0.24 while in the corresponding hexa-aza macrocyclic complex, the water molecule forms only weak hydrogen bonds with L_2 forming a hydrated complex $[Ni^{III}L_2(SO_4)]^+.(H_2O)$.[8] The weak bonding of water in $[Ni^{III}L_2(SO_4)]^+.(H_2O)$ explains its faster kinetics towards hydrogen peroxide oxidation as compared to $[Ni^{III}L_1(SO_4)(H_2O)]^+$. In contrast, the present study reveals that the acetate ligand is axially coordinated in both $[Ni^{III}L_1(SO_4)(OAc)]$ and $[Ni^{III}L_2(SO_4)(OAc)]$ with similar bond strength. The DFT study reveals that the coordinate bonds between Ni(III) and the equatorial as well as axial ligands in $[Ni^{III}L_1(SO_4)(OAc)]$ and $[Ni^{III}L_2(SO_4)(OAc)]$ are very similar. The presence of the strong H-bond between the sulphate and the pendant OH of L_2 confers additional stability to $[Ni^{III}L_2(SO_4)(OAc)]$ as compared to $[Ni^{III}L_1(SO_4)(OAc)]$. This explains the observed faster rate of oxidation of hydrogen peroxide by $[Ni^{III}L_1(SO_4)(OAc)]$.

It was pointed out that upon one-electron oxidation or reduction of the complexes of the type $[Fe^{II}Cl(cyclam\text{-}OAc)]$, the O-coordinated carboxylate would not dissociate.[18] Thus, the stability and hence the reactivity of the Ni(III) complexes can be reviewed on the basis of acidity of hydrogen bound to the secondary nitrogen of macrocylic ligands. In both $[Ni^{III}L]$ complexes, hydrogen bonding is formed between secondary hydrogen of L and oxygen of acetate and sulphate ligands. It was reported that in perchlorate media above pH 2, $[Ni^{III}(L_1)(H_2O)_2]^{3+}$ decomposes rapidly *via* $[Ni(L_1)(OH)(H_2O)]$ and very short-lived pink solution probably containing $Ni^{III}L(OH)^{2+}$ or $Ni^{III}L$ was formed.[44] On quenching with an acidic sulphate solution yielded $Ni^{III}L(SO_4)^{2-}$. On the other hand, $[Ni^{III}L_2]$ complexes do not show dehydrogenation of macrocyclic ligand even in basic medium.[23] In our previous reports, we studied the oxidation of Ni(II) macrocylic complexes by hydrogen peroxide and *t*-Butyl hydroperoxide in detail.[7,8] When $[Ni^{II}L_1]$ reacts with H_2O_2, oxidation of macrocylic ring takes place by the abstraction of hydrogen atom of secondary nitrogen by $^{\bullet}OH$. The reaction leads to the formation of tetraene form of dimer by the removal of an α-hydrogen. In the case of $Ni^{II}L_2$, the α-position is strained due to the uncoordinated bridge head nitrogen with hydroxyl ethyl substituent so that it forms only diene. From these results, we suggest that the lower acidity of secondary hydrogens of hexa-aza macrocylic ligand and H-bond formation between pendent –OH group of hexa-aza macrocylic ligand and sulphato oxygen play an effective role in the stabilization of the $[Ni^{III}L_2]$ complex at pH > 3. Thus, this study explains the stability of $[Ni^{III}L_2]$ complex at higher pH.

4. Conclusions

The effect of axial acetate ligand in stabilising Ni(III) tetra-aza and hexa-aza complexes is studied by carrying out oxidation of hydrogen peroxide in aqueous medium. The reaction was catalysed by Cu(II) to retard the ligand oxidation. The rate of decomposition of hydrogen peroxide by $[Ni^{III}L_1(SO_4)(OAc)]$ is faster than that by $[Ni^{III}L_2(SO_4)(OAc)]$. The DFT study shows that the acetate anion coordination to Ni(III) is stronger than that of the sulphate ligand in aqueous medium as revealed by the computed Ni–O(OAc) and Ni–O(SO_4) covalent bond orders. The gas-phase calculations also show that both sulphate and acetate are axially coordinated in $[Ni^{III}L_1(SO_4)(OAc)]$ and $[Ni^{III}L_2(SO_4)(OAc)]$. However, in the gas-phase, the sulphate ligand is predicted to be stronger than the acetate ligand. The stability of $[Ni^{III}L_2]$ in pH > 3 is due to the uncoordinated bridge head nitrogen providing more strain in the α-position and the formation of hydrogen bond between pendent –OH of macrocyclic ligand and sulphato oxygen. This study again provides experimental support to the fact that the hydroxyl groups in $[Ni^{III}L_2]$ are inert in basic medium.

Supplementary Information (SI)

The complete optimized geometries of Ni(III) macrocyclic complexes, **1** [$Ni^{III}L_1(SO_4)(OAc)$] and **2** [$Ni^{III}L_2(SO_4)(OAc)$] (Figure S1), Cartesian Coordinates (in Å) of BP86/def2-TZVP optimized geometries and BP86/TZVP gas-phase optimized Cartesian coordinates are available at www.ias.ac.in/chemsci.

References

1. Telser J, Horng Y C, Becker D F, Hoffman B M and Ragsdale S W 2000 On the Assignment of Nickel Oxidation States of the Ox1, Ox2 Forms of Methyl-Coenzyme M Reductase *J. Am. Chem. Soc.* **122** 182
2. Hunter T M, McNae I W, Simpson D P, Smith A M, Moggach S, White F, Walkinshaw M D, Parsons S and Sadler P J 2007 Configuration of Nickel-Cyclam Antiviral Complexes and Protein Recognition *Chem. Eur. J.* **13** 40
3. Cho J, Sarangi R, Annaraj J, Kim S Y, Kubo M, Ogura T, Solomon E I and Nam W 2009 Geometric and electronic structure and reactivity of a mononuclear "side-on" nickel(III)-peroxo complex *Nature Chem.* **1** 568
4. (a) Zilbermann I, Meshulam A, Cohen H and Mayerstein D 1993 Stabilization of nickel(III)-1,8-dimethyl-1,3,6,8,10,13-hexaazacyclotetradecane by axial binding of anions in neutral aqueous solutions *Inorg. Chim. Acta* **206** 127; (b) Shamir D, Zilbermann I, Maimon E, Shames A I, Cohen H and Meyerstein D 2010 Anions as stabilizing ligands for Ni(III)(cyclam) in aqueous solutions *Inorg. Chim. Acta* **363** 2819
5. Burg Ariela, Maimon Eric, Cohen H and Meyerstein D 2007 Ligand Effects on the Chemical Activity of Copper(I) Complexes: Outer- and Inner-Sphere Oxidation of $Cu^{I}L$ *Eur. J. Inorg. Chem.* 530
6. Anuradha S and Vijayaraghavan V R 2010 Kinetics of oxidation of benzenediols by (1,8-bis(2-hydroxyethyl)-1,3,6,8,10,13-hexaazacyclotetradecane) nickel(III) in aqueous acidic media *React. Kinet. Mech. Cat.* **101** 279
7. Anuradha S and Vijayaraghavan V R 2013 Oxidation of hydrogen peroxide by $[Ni^{III}(cyclam)]^{3+}$ in aqueous acidic media *J. Chem. Sci.* **125** 1123
8. Anuradha S, Malar E J P and Vijayaraghavan V R 2015 Kinetic measurements and quantum chemical calculations on low spin Ni(II)/(III) macrocyclic complexes in aqueous and sulphato medium *J. Chem. Sci.* **127** 1287
9. Choi H J, Lee T S and Suh M P 1999 Self-Assembly of a Molecular Floral Lace with One-Dimensional Channels and inclusion of Glucose *Angew. Chem. Int. Ed.* 1405
10. Choi K Y, Ryu H, Lee K C, Lee H H, Hong C P, Kim J H and Sung N D 2003 One-Dimensional Hydrogen-Bonded Infinite Chains Composed of a Nickel(II) Macrocyclic Complex and Organic ligands *Bull. Korean. Chem. Soc.* **24** 1150
11. Kim J C, Lough A J and Kim H 2002 Structurally different nickel(II) hexaaza macrocyclic complexes with the same btc^{2-} anions (btc^{2-} = 1,2,4,5-benzenetetracarboxylic acid dianion *Inorg. Chem. Commun.* **5** 771
12. Choi K Y, Suh I H and Hong C P 1999 A novel one-dimensional nickel(II) complex with a hydrogen-bond-link *Inorg. Chem. Commun.* **2** 604
13. Lindoy L F, Mahinay M S, Skelton B W and White A H 2003 Ligand assembly and metal ion complexation: Synthesis and X-ray structures of Ni(II) and Cu(II) benzoate and 4-tert-butylbenzoate complexes of cyclam *J. Coord. Chem.* **56** 1203
14. Macartney D H 1986 The oxidation of hydrogen peroxide by tris(polypyridne)complexes of osmium(III), iron(III), ruthenium(III), and nickel(III) in aqueous media *Can. J. Chem.* **64** 1936
15. Koshino N, Funahashi S and Takagi H D 1997 Oxidation of hydrogen peroxide by bis(1,4,7-triazacyclononane)nickel(III), bis(1,4,7-trithiacyclononane)iron(III) and tris(2,2′-bipyridine)ruthenium(III) ions in acidic aqueous solutions *J. Chem. Soc., Dalton Trans.* 4175
16. Reger D L, Debreczeni A, Smith M D, Jezierska J and Ozarowski A 2012 Copper(II) Carboxylate Dimers Prepared from Ligands Designed to Form a Robust $\pi \ldots \pi$ Stacking Synthon: Supramolecular Structures and Molecular Properties *Inorg. Chem.* **51** 1068
17. Esparza-Ruiz A, Peña-Hueso A, Mijangos E, Osorio-Monreal G, Nöth H, Flores-Parra A, Contreras R and Barba-Behrens N 2011 Cobalt(II), nickel(II) and zinc(II) coordination compounds derived from aromatic amines *Polyhedron* **30** 2090
18. Serres R G, Grapperhaus C A, Bothe E, Bill E, Weyhermüller T, Neese F and Wieghardt K 2004 Structural, Spectroscopic, and Computational Study of an Octahedral, Non-Heme$\{Fe\text{-}NO\}^{6-8}$ Series: $[Fe(NO)(cyclam\text{-}ac)]^{2+/+/0}$ *J. Am. Chem. Soc.* **126** 5138
19. Aliaga-Alcalde N, George S D, Mienert B, Bill E, Wieghardt K and Neese F 2005 The Geometric and Electronic Structure of $[(cyclam\text{-}acetato)Fe(N)]^{+}$: A Genuine Iron(v) Species with a Ground-State Spin S = ** *Bio. Inorg. Chem. Angew. Chem. Int. Ed.* **44** 2908
20. Barefield E K, Wagner F, Herlinger A W and Dahl A R 1979 (1,4,8,11-Tetraazacyclotetradecane)Nickel(II) Perchlorate and 1,4,8,11-Tetraazacyclotetradecane *Inorg. Synth.* **16** 220
21. McAuley A, Palmer T A and Whitcombe T W 1993 X-ray crystal structure of $[Ni(III)(cyclam)(NO_3)_2](ClO_4)$ and electron transfer reactions of the Ni(III)/Ni(II) couple *Can. J. Chem.* **71** 1792
22. Suh M P, Shim B Y and Yoon T 1994 Template Synthesis and Crystal Structures of Nickel(II) Complexes of Hexaaza Macrocyclic Ligands with Pendant Functional Groups: Formation of a Coordination Polymer *Inorg. Chem.* **33** 5509
23. Suh M P, Lee E Y and Shim B Y 1998 Synthesis and properties of nickel(III) complexes of hexaazamacrocylic ligands *Inorg. Chim. Acta* **269** 337
24. Espenson J H 1995 In *Chemical Kinetics and Reaction Mechanisms* 2nd ed. (McGraw-Hill)
25. (a) Becke A D 1988 Density-functional exchange-energy approximation with correct asymptotic behaviour *Phys. Rev. A* **38** 3098; (b) Perdew J P 1986 Density functional approximation for the correlation energy of the inhomogeneous electron gas *Phys. Rev. B* **33** 8822

26. Weigend F and Ahlrichs R 2005 Balanced basis sets of split valence, triple zeta valence and quadruple zeta valence quality for H to Rn: Design and assessment of accuracy *Phys. Chem. Chem. Phys.* **7** 3297
27. Schweinfurth D, Krzystek J, Schapiro I, Demeshko S, Klein J, Telser J, Ozarowski A, Su C Y, Meyer F, Atanasov M, Neese F and Sarkar B 2013 Electronic Structures of Octahedral Ni(II) Complexes with "Click" Derived Triazole Ligands: A Combined Structural, Magnetometric, Spectroscopic, and Theoretical Study *Inorg. Chem.* **52** 6880
28. Petrenko T, Ray K, Wieghardt K E and Neese F 2006 Vibrational Markers for the Open-Shell Character of Transition Metal Bis-dithiolenes: An Infrared, Resonance Raman, and Quantum Chemical Study *J. Am. Chem. Soc.* **128** 4422
29. Izsak R and Neese F 2011 An overlap fitted chain of spheres exchange method *J. Chem. Phys.* **135** 144105
30. Kossmann S and Neese F 2010 Efficient Structure Optimization with Second-Order Many-Body Perturbation Theory: The RIJCOSX-MP2 Method *J. Chem. Theory Comput.* **6** 2325
31. Kossmann S and Neese F 2009 Comparison of two efficient approximate Hartree-Fock approaches *Chem. Phys. Lett.* **481** 240
32. Neese F, Wennmohs F, Hansen A and Becker U 2009 Efficient approximate and parallel Hartree-Fock hybrid DFT calculations. A 'chain-of-spheres' algorithm for the Hartree-Fock exchange *Chem. Phys.* **356** 98
33. Neese F 2003 An improvement of the resolution of the identity approximation for the formation of the coulomb matrix *J. Comp. Chem.* **24** 1740
34. Neese F 2012 The ORCA program system Wiley Interdiscip *Rev.*: *Comput. Mol. Sci.* **2** 73
35. Klamt A and Schüürmann G 1993 COSMO: A new approach to dielectric screening in solvents with explicit expressions for the screening energy and its gradient *J. Chem. Soc.*, *Perkin Trans.* **2** 799
36. (a) Grimme S, Antony J, Ehrlich S and Krieg H 2010 A consistent and accurate *ab initio* parametrization of density functional dispersion correction (DFT-D) for the 94 elements H-Pu *J. Chem. Phys.* **132** 154104; (b) Grimme S 2011 Density functional theory with London dispersion corrections Wiley Interdiscip. *Rev.*: *Comput. Mol. Sci.* **1** 211
37. (a) Mayer I 1983 Charge, bond order and valence in the *ab initio* SCF theory *Chem. Phys. Lett.* **97** 270; (b) Mayer I 1984 Bond order and valence: Relations to Mulliken's population analysis *Int. J. Quant. Chem.* **26** 151; (c) Mayer I 1985 Bond orders and valences in the SCF theory: A comment *Theor. Chim. Acta* **67** 315
38. Frisch M J *et al.* 2004 In *GAUSSIAN 03*, Revision E.01 (Wallingford CT: Gaussian Inc.)
39. Malar E J P 2004 Can the cyclo-P_5 Ligand Introduce Basicity at the Transition Metal Center in Metallocenes? A Hybride Density Functional Study on the cyclo-P_5 Analogues of Metallocenes of Fe, Ru and Os *Eur. J. Inorg. Chem.* 2723
40. Malar E J P 2005 Density functional theory analysis of some triple-decker sandwich complexes of iron containing cyclo-P_5 and cyclo-As_5 ligands *Theoret. Chem. Acc.* **114** 213
41. Malar E J P 2003 Do Penta- and Decaphospha Analogues of Lithocene Anion and Beryllocene Exist? Analysis of Stability, Structure, and Bonding by Hybride Density Functional Study *Inorg. Chem.* **42** 3873
42. Calvi A O, Aullon G, Alvarez S, Montero L A and Stohrer W D 2006 Bonding and solvation preferences of nickel complexes $[Ni(S_2PR_2)_2]$ (R=H, Me, OMe) according a natural bond orbital analysis *J. Mol. Structure*: *Theochem.* **767** 37
43. Arunan E, Desiraju G R, Klein R A, Sadlej J, Scheiner S, Alkorta I, Clary D C, Crabtree R H, Dannenberg J J, Hobza P, Kjaergaard H G, Legon A C, Mennucci B and Nesbitt D J 2011 Defining the hydrogen bond: An account (IUPAC Technical Report) *Pure Appl. Chem.* **83** 1619
44. Zeigerson E, Bar I, Bernstein J, Kirschenbaum L J and Meyerstein D 1982 Stabilization of the tervalent nickel complex with meso-5,7,7,12,14,14-hexamethyl-1,4,8,11-tetraazacyclotetradecane by axial coordination of anions in aqueous solution *Inorg. Chem.* **21** 73